Biochimica et Biophysica Acta 1848 (2015) 634–642

Contents lists available at ScienceDirect

Biochimica et Biophysica Acta

journal homepage: www.elsevier.com/locate/bbamem

Scolopendin 2, a cationic antimicrobial peptide from centipede, and its membrane-active mechanism

Heejeong Lee [a,1], Jae-Sam Hwang [b,1], Jaeho Lee [c], Jae Il Kim [c], Dong Gun Lee [a,*]

[a] School of Life Sciences, BK 21 Plus KNU Creative BioResearch Group, College of Natural Sciences, Kyungpook National University, Daehak-ro 80, Buk-gu, Daegu 702-701, Republic of Korea
[b] Department of Agricultural Biology, National Academy of Agricultural Science, RDA, Jeonju, Republic of Korea
[c] School of Life Sciences, Gwangju Institute of Science and Technology, Oryong-dong, Buk-gu, Gwangju 500-712, Republic of Korea

ARTICLE INFO

Article history:
Received 10 June 2014
Received in revised form 4 November 2014
Accepted 17 November 2014
Available online 22 November 2014

Keywords:
Scolopendin 2
Scolopendra subspinipes mutilans
Antimicrobial peptide
Membrane damage

ABSTRACT

Scolopendin 2 is a 16-mer peptide (AGLQFPVGRIGRLLRK) derived from the centipede *Scolopendra subspinipes mutilans*. We observed that this peptide exhibited antimicrobial activity in a salt-dependent manner against various fungal and bacterial pathogens and showed no hemolytic effect in the range of 1.6 μM to 100 μM. Circular dichroism analysis showed that the peptide has an α-helical properties. Furthermore, we determined the mechanism(s) of action using flow cytometry and by investigating the release of intracellular potassium. The results showed that the peptide permeabilized the membranes of *Escherichia coli* O157 and *Candida albicans*, resulting in loss of intracellular potassium ions. Additionally, bis-(1,3-dibutylbarbituric acid) trimethine oxonol and 3,3′-dipropylthiacarbocyanine iodide assays showed that the peptide caused membrane depolarization. Using giant unilamellar vesicles encapsulating calcein and large unilamellar vesicles containing fluorescein isothiocyanate-dextran, which were similar in composition to typical *E. coli* O157 and *C. albicans* membranes, we demonstrated that scolopendin 2 disrupts membranes, resulting in a pore size between 4.8 nm and 5.0 nm. Thus, we have demonstrated that a cationic antimicrobial peptide, scolopendin 2, exerts its broad-spectrum antimicrobial effects by forming pores in the cell membrane.

1. Introduction

Microbial resistance to antibiotics has increased in recent years, resulting in the invalidation of major antimicrobial drugs used in clinical settings [1]. Resistance to various antibiotics may be due to failure of the drug to interact with its target, efflux of the antibiotic from the cell, or direct destruction or modification of the drug [2,3]. The discovery of novel, broad-spectrum antibiotics with rapid antimicrobial effects and the ability to limit the induction of microbial resistance may not keep up with the pace at which pathogens are developing resistance [4,5].

One way to overcome the problem of antibiotic resistance is to use antimicrobial peptides (AMPs), which can be isolated from natural sources and are effective against a broad range of microorganisms, including Gram-positive and Gram-negative bacteria, fungi, and viruses [4]. AMPs play a significant role in the defense systems of higher organisms such as plants, insects, arthropods, amphibians, and mammals [6]. Cell viability is maintained by preserving the structure of the cell wall or cytoplasmic membrane, regardless of DNA/protein inhibition by single or dual mechanism(s). While their antimicrobial properties have only recently been identified, AMPs have received attention as novel chemotherapeutics, intracellular signaling molecules, and antitumor agents [5].

AMPs from venom, such as melittin from bees and hadrurin from scorpions, have been reported previously [6,7]. Centipedes are venomous arthropods that have been used in traditional medicine to treat several ailments, including carbuncles and neoplasms [8]. Extracts from centipedes have been reported to contain antibacterial components and toxins with anticoagulant properties [6]. In a previous study, we identified an antimicrobial peptide, scolopendin 1, from the centipede *Scolopendra subspinipes mutilans* [9]. Other antimicrobial peptides from this species, such as scolopin 1 and 2 and FXa-inhibiting peptide, have also been reported [9–11]. In this study, we identified an antimicrobial peptide from *S. s. mutilans* and investigated its antimicrobial properties.

Abbreviations: AMPs, antimicrobial peptides; SmAE, *S. s. mutilans* Assembled EST; ATCC, American Type Culture Collection; KCTC, Korean Collection for Type Cultures; MIC, minimum inhibitory concentration; PBS, phosphate-buffered saline; CD, circular dichroism; TFE, trifluoroethanol; DPC, diphosphocholine; $DiBAC_4(3)$, bis-(1,3-dibutylbarbituric acid) trimethine oxonol; $DiSC_3(5)$, 3,3′-dipropylthiacarbocyanine iodide; GUV, giant unilamellar vesicle; PE, phosphatidylethanolamine; PG, phosphatidylglycerol; PC, phosphatidylcholine; PI, phosphatidylinositol; LUV, large unilamellar vesicle

* Corresponding author. Tel.: +82 53 950 5373; fax: +82 53 955 5522.
E-mail address: dglee222@knu.ac.kr (D.G. Lee).

[1] These authors contributed equally to this work and should be considered co-first authors.

http://dx.doi.org/10.1016/j.bbamem.2014.11.016
0005-2736/

2. Materials and methods

2.1. Transcriptome sequencing

Centipedes were injected with exponential-phase *Escherichia coli* (2×10^6 colony forming units (CFU)/centipede). Eighteen hours later, total RNA was isolated from the centipedes using the RNeasy Total RNA Isolation Kit (Qiagen, USA). The integrity of RNA was verified using an Agilent 2100 Bioanalyzer. Poly(A) mRNA was isolated using oligo(dT) beads. Short mRNA fragments were obtained by adding fragmentation buffer, and first- and second-strand cDNA was synthesized in succession. Short fragments were purified using the QIAquick PCR Purification Kit, end repair was performed, and a poly(A) tail adapter sequence was added. Suitable amplified fragments were selected as templates using the agarose gel electrophoresis method. Finally, the library was sequenced on an Illumina HiSeq™ 2000 System by generating paired-end libraries with an average insert size of 200 bp, following the manufacturer's instructions.

2.2. Assembly, screening based on physicochemical properties and selection of an AMP

The *S. s. mutilans* transcriptome was assembled *de novo*, without a reference genome, using the Trinity method [13]. Sequences that could not be extended on either end were acquired using TGICL software [14]. The resulting sequences (contigs and singletons), referred to as *S. s. mutilans* Assembled EST (SmAE) sequences, were translated into amino acid sequences with ESTScan [15]. These amino acid sequences were screened for potential AMPs based on physicochemical properties of known AMPs using EMBOSS PEPSTATS [16]. AMPs were then selected based on sequence similarity with known AMPs, determined using BLASTx. Among the putative AMPs thus obtained, the following AMP was synthesized: scolopendin 2. Peptide synthesis was performed by Anygen Co. (Gwangju, Korea).

2.3. Circular dichroism spectroscopy

Circular dichroism (CD) spectra of the peptides were recorded using a Jasco J-710 CD spectrophotometer (Jasco, Tokyo, Japan) with a 1-mm path length cell. CD was measured at wavelengths from 195 nm to 240 nm (bandwidth, 1 nm; step resolution, 0.1 nm; speed, 50 nm/min; response time, 0.5 s). CD spectra were recorded for the peptides in the presence of phosphate-buffered saline (PBS), 50% trifluoroethanol (TFE), 50 mM SDS micelles, and 0–5 mM diphosphocholine (DPC) (pH 7.4) at 20 °C. The spectra were averaged over three scans [17].

2.4. Microbial strains

Enterococcus faecium (ATCC 19434), *Staphylococcus aureus* (ATCC 25923), *E. coli* O157 (ATCC 43895), *Salmonella typhi* (ATCC 19430), *Pseudomonas aeruginosa* (ATCC 27853), *Candida albicans* (ATCC 90028), and *Candida parapsilosis* (ATCC 22019) were obtained from the American Type Culture Collection (ATCC) (Manassas, VA, USA). *Trichosporon beigelii* (KCTC 7707) and *Trichophyton rubrum* (KCTC 6345) were obtained from the Korean Collection for Type Cultures (KCTC). Methicillin-resistant *S. aureus* and antibiotic-resistant *P. aeruginosa* were obtained from a tertiary teaching hospital in Daegu, South Korea. The isolates were processed by the MicroScan WalkAway 96 system for genus and species identification. The susceptibility of resistant strains to antimicrobial agents was tested using MicroScan Gram positive MIC/combo (PC1A), Gram negative MIC/combo (NC44) and Gram negative breakpoint combo (NBC39) panels [18].

2.5. Antimicrobial activity

The bacterial strains were cultured in Luria-Bertani (LB) broth (Difco) with aeration at 37 °C and the fungal strains were cultured in yeast extract–peptone–dextrose (YPD) broth (Difco) with aeration at 28 °C. Optical density was measured with a spectrophotometer (DU530, Beckman, Fullerton, CA, USA) and cell cultures were adjusted to obtain standardized populations. Cells in the exponential phase (2×10^6 cells/mL) were dispensed into wells of microtiter plates (0.1 mL/well). Minimum inhibitory concentration (MIC) was determined using two-fold serial dilutions of the test peptides, based on the Clinical and Laboratory Standards Institute (CLSI) method [19]. The MIC values were determined from three independent tests.

2.6. Hemolytic activity

The hemolytic activity of the peptides was evaluated by determining the release of hemoglobin from a 4% suspension of human erythrocytes, measured at 414 nm with an ELISA reader. Hemolytic levels of 0 and 100% were determined in PBS (35 mM phosphate buffer, 150 mM NaCl, pH 7.4) and with 0.1% Triton X-100, respectively. Percent hemolysis was calculated as follows: hemolysis (%) = [($Abs_{414\ nm}$ in the peptide solution − $Abs_{414\ nm}$ in PBS) / ($Abs_{414\ nm}$ in 0.1% Triton X-100 − $Abs_{414\ nm}$ in PBS)] × 100 [20].

2.7. Permeability of microbial cells

E. coli O157 and *C. albicans* cells in the log phase (2×10^6 cells/mL) were suspended in PBS and treated with the MICs of the peptides. After incubation for 4 h at 37 °C and 28 °C, respectively, the cells were harvested by centrifugation and resuspended in PBS. Subsequently, the cells were treated with 1 μM SYTOX Green. The cells were analyzed with a FACSCalibur flow cytometer (Becton Dickinson, San Jose, CA, USA) [21].

2.8. Membrane depolarization

Log-phase cells of *E. coli* O157 and *C. albicans* (2×10^6 cells/mL) were harvested and resuspended in PBS. After incubation with the MICs of the peptides for 4 h at 37 °C and 28 °C, respectively, the cells were again harvested by centrifugation and resuspended in PBS. Subsequently, the cells were treated with 50 μg/mL bis-(1,3-dibutylbarbituric acid) trimethine oxonol [$DiBAC_4(3)$] (Molecular Probes, Eugene, OR, USA). Flow cytometric analysis was performed using a FACSCalibur flow cytometer [22].

E. coli O157 cells were harvested by centrifugation (3500 rpm, 7 min), washed in 5 mM HEPES buffer (pH 7.2) containing 20 mM glucose, and resuspended in buffer (5 mM HEPES buffer, 20 mM glucose, 100 mM KCl, pH 7.2) to an OD_{600} of 0.05. Harvested *C. albicans* cells (2×10^6 cells/mL) were washed with Ca^{2+}- and Mg^{2+}-free PBS. Changes in the membrane potential were measured using a membrane-potential-sensitive probe, 3,3′-dipropylthiacarbocyanine iodide [$DiSC_3(5)$]. To determine the effect of salt, the cells were treated with peptide (at the MIC) under various salt conditions (final concentrations: 150 mM NaCl and 1 mM $MgCl_2$). Changes in fluorescence due to the collapse of the cytoplasmic membrane potential were monitored continuously using a spectrofluorophotometer (Shimadzu, RF-5301PC, Shimadzu, Kyoto, Japan) at an excitation wavelength of 622 nm and an emission wavelength of 670 nm. The experiment was repeated three times under each condition to ensure reproducibility [23,24].

2.9. Leakage of potassium

The antimicrobial activity of the peptides was analyzed by measuring the efflux of potassium ions from *E. coli* O157 and *C. albicans* cells using an ISE meter (Orion Star A214, Thermo Scientific, Singapore).

```
                                    10
Scolopendin 2  :    -----AGLQFP-VG---R-I-G-RLLRK---      -COOH   :      16
  Buforin 2    :   TRSSRAGLQFP-VG---R-V-H-RLLRK---      -COOH   :      21
Temporin-1ARa  :    ------FL--PIVGRLIS---G--LL-----      -COOH   :      13
Temporin-AJ8   :    --------FFPIVGKRLY---G--LL-----      -COOH   :      16
Temporin-CPb   :    ------FL--PIVGRLIS---G--IL-----      -COOH   :      16
  CPF-AM4      :    ------GLGSL-VGNALR-I-GAKLL-----      -COOH   :      16
```

Fig. 1. Alignment of amino acid sequences of scolopendin 2, buforin 2, temporins, and CPF-AM4.

The two cell suspensions (2×10^6 cells/mL) were incubated with peptide for 4 h at 37 °C and 28 °C, respectively. The incubated cells were then centrifuged at 12,000 rpm for 5 min to remove cell debris. The potassium ion concentration in the supernatant was expressed as a percentage of the total free potassium, which was determined following sonication of the cells [25,26].

2.10. Calcein leakage from giant unilamellar vesicles

Giant unilamellar vesicles (GUVs) with encapsulated calcein were prepared using indium tin oxide (ITO)-coated glass slides. The following lipid mixtures were prepared at a concentration of 3.75 mg/mL in chloroform: phosphatidylethanolamine (PE)/phosphatidylglycerol (PG) (3:1, w/w) and phosphatidylcholine (PC)/PE/phosphatidylinositol (PI)/ergosterol (5:4:1:2, w/w/w/w) [27]. PE was L-α-phosphatidylethanolamine from egg yolk, Type III (P7943, Sigma). PG was L-α-phosphatidyl-DL-glycerol sodium salt from egg yolk lecithin (P8318, Sigma). PC was L-α-phosphatidylcholine from egg yolk, Type XVI-E (Sigma) that has fatty acid contents of approximately 33% 16:0 (palmitic), 13% 18:0 (stearic), 31% 18:1 (oleic), and 15% 18:2 (linoleic) (other fatty acids being minor contributors). PI was L-α-phosphatidylinositol from Glycine max (soybean) (P6636, Sigma). Acyl chain compositions of phospholipid used were composed of saturated or unsaturated fatty acid part. The lipid mixtures (200 μL) were spread onto ITO-coated glass in a spin coater (Spin coater, ACE-1020 Series) at 500 rpm for 5 min. The lipid-coated ITO glass was subjected to evaporation under vacuum for 3 h. Lipid-coated and uncoated glass slides were placed facing each other with a 2-mm-thick Teflon spacer between them. The chamber was filled with buffer (10 mM HEPES buffer, pH 7.2, 10 μM. glucose, 1 mM calcein), and an alternating voltage with an amplitude of 1.7 V (peak-to-peak, sine wave) and frequency of 10 Hz was applied to the ITO electrodes using a sweep function generator (SWEEP FUNCTION GENERATOR 9205C, Protek) for 2 h. The voltage across the ITO glass was changed to 4 V (peak-to-peak) at 4 Hz for 10 min. Gel filtration chromatography on a Sephadex G-50 column was used to remove free calcein from the calcein-containing GUVs. The GUVs were treated with the peptides and changes were observed with an inverted fluorescence microscope (Eclipse Ti-S, Nikon, Japan) [28,29].

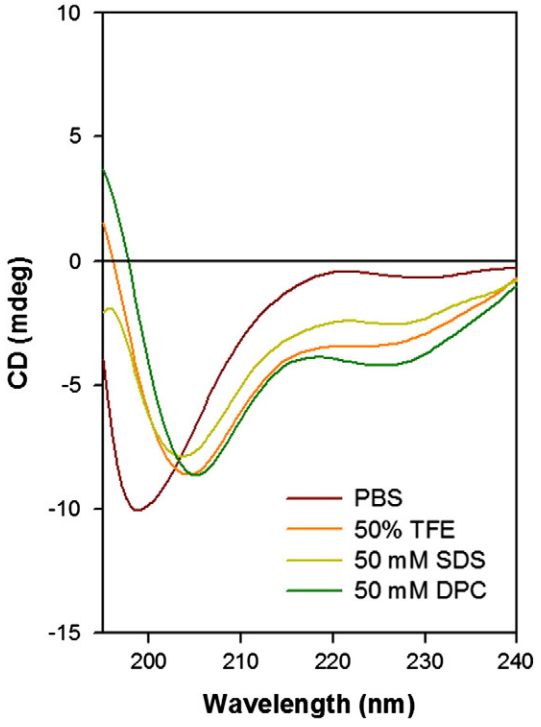

Fig. 2. Circular dichroism spectra of scolopendin 2 (50 μM) in the presence of PBS, 50% TFE, 50 mM SDS, and 50 mM DPC (pH 7.4).

2.11. FITC-dextran leakage from large unilamellar vesicles

To prepare large unilamellar vesicles (LUVs) containing fluorescein isothiocyanate-labeled dextrans (FITC-dextran) with average molecular weights of 4000, 10,000, 20,000, 40,000, and 70,000 (FD 4, FD 10, FD 20, FD 40, and FD 70), lipid mixtures of the same composition to the GUVs were evaporated, hydrated in dye buffer solution (10 mM Tris, 150 mM NaCl, and 0.1 mM EDTA, pH 7.4), and mixed with each FD. The suspensions were subjected to 13 freeze–thaw cycles and extruded through two stacked polycarbonate filters (200-nm pores) with a LiposoFast extruder (Avestin Inc., Ottawa, Canada). Gel filtration chromatography on a Sephadex G-50 column was performed to separate LUVs from free dye. Dye leakage from the LUVs was monitored by measuring the intensity of fluorescence at an excitation wavelength of 494 nm and an emission wavelength of 520 nm using a spectrofluorophotometer (Shimadzu, RF-5301PC, Shimadzu, Kyoto, Japan), while 1% Triton X-100 was used to determine 100% dye release. The percent

Table 1
The antimicrobial activity of scolopendin 2, BUF(6–21) and melittin.

Microbial strains	MIC (μM)		
	Scolopendin 2	BUF(6–21)	Melittin
Gram-positive bacteria			
E. faecium ATCC 19434	12.5	25.0	3.1
S. aureus ATCC 25923	25.0	25.0	1.6
MRSA 1	12.5	12.5	3.1
MRSA 2	12.5	25.0	3.1
MRSA 3	12.5	25.0	1.6
Gram-negative bacteria			
E. coli O157 ATCC 43895	6.3	6.3	3.1
S. typhi ATCC 19430	12.5	6.3	1.6
P. aeruginosa ATCC 27853	12.5	12.5	3.1
ARPA 1	6.3	6.3	1.6
ARPA 2	12.5	6.3	1.6
ARPA 3	12.5	12.5	3.1
Fungal strains			
C. albicans ATCC 90028	6.3	12.5	3.1
C. parapsilosis ATCC 22019	12.5	25.0	3.1
T. beigelii KCTC 7707	6.3	12.5	3.1
T. rubrum KCTC 6345	6.3	12.5	6.3

E. faecium: *Enterococcus faecium*, *S. aureus*: *Staphylococcus aureus*, MRSA: methicillin-resistant *Staphylococcus aureus*, *E. coli*: *Escherichia coli* O157, *S. typhi*: *Salmonella typhi*, ARPA: antibiotics-resistant *Pseudomonas aeruginosa*, *C. albicans*: *Candida albicans*, *C. parapsilosis*: *Candida parapsilosis*, *T. beigelii*: *Trichosporon beigelii*, *T. rubrum*: *Trichophyton rubrum*.

Table 2
Human erythrocyte lysis assay against scolopendin 2, BUF(6–21) and melittin.

Peptides	Hemolysis (%)						
	100.0 μM	50.0 μM	25.0 μM	12.5 μM	6.3 μM	3.1 μM	1.6 μM
Scolopendin 2	0 ± 0.2	0 ± 0.3	0 ± 0.5	0 ± 0.4	0 ± 0.4	0 ± 0.3	0 ± 0.8
BUF(6–21)	0 ± 0.4	0 ± 0.2	0 ± 0.1	0 ± 0.3	0 ± 0.5	0 ± 0.7	0 ± 0.6
Melittin	100 ± 3.6	100 ± 2.8	100 ± 7.2	100 ± 6.1	75.3 ± 5.7	42.9 ± 6.7	12.3 ± 4.2

dye leakage caused by the peptides was calculated as follows: dye leakage (%) = 100 × ($F - F_0$) / ($F_t - F_0$), where F represents the fluorescence intensity achieved after addition of the peptides and F_0 and F_t represent the fluorescence intensities without any compound and with Triton X-100, respectively [30]. The data represent the mean ± standard deviation of three independent experiments.

3. Results

3.1. Characterization and antimicrobial activity of scolopendin 2

The transcriptome of the centipede *S. s. mutilans* was sequenced, and corresponding peptide sequences were acquired. Following sequential BLAST analysis of these peptide sequences to determine similarity with known AMP sequences, a cationic AMP was selected and synthesized. The amino acid sequence of the selected peptide, termed scolopendin 2, was AGLQFPVGRIGRLLRK. The purity and observed molecular mass of the synthesized peptide were 99.6% and 1780.4 Da (calculated mass = 1781.2 Da), respectively. The net charge at physiological pH was +4. Scolopendin 2 has sequence similarity with previously reported AMPs such as buforin 2, temporins, and CPF-AM4 [5,31,32]. The highest homology was observed with buforin 2 (66.7%), whereas the similarity with temporin-1ARa, temporin-AJ8, temporin-CPb, and CPF-AM4 was 42.7%, 45.0%, 42.1%, and 42.1%, respectively (Fig. 1). In particular, scolopendin 2 is very similar to buforin 2, and is almost identical to residues 6–21 in that peptide, BUF(6–21). The peptides has the same length and differ only at two positions, I15V and G16H. The antimicrobial activity of BUF(6–21) was reported but the mechanism was not yet studied [31]. Based on these sequence similarities with potent antimicrobial peptides, we hypothesized that scolopendin 2 also possesses antimicrobial properties. To investigate alterations of the secondary structure of the peptide, CD spectroscopy was conducted in PBS with or without TFE, SDS, and DPC. As shown in Fig. 2, the results indicate that the peptide has an α-helical properties in membrane-like conditions but a random coil pattern in PBS.

To investigate the antimicrobial effect of scolopendin 2, a MIC test was performed against several pathogenic and antibiotic-resistant strains of bacteria and fungi. Melittin, having broad-spectrum antimicrobial activity [33], and BUF(6–21), having high similarity [31], was used as control peptides. As shown in Table 1, scolopendin 2 had antimicrobial activity, with MIC values in the range of 6.3 to 25.0 μM. BUF(6-21) showed a similar antimicrobial activity, with a slightly lower activity than scolopendin 2, but always within one dilution factor. Melittin, with MIC values in the range of 3.1 to 6.3 μM, was more potent than scolopendin 2. However, scolopendin 2 and BUF(6–21) showed no hemolytic activity towards human erythrocytes, at any concentration (Table 2). These results indicate that scolopendin 2 has potential as an AMP with no hemolytic effect.

3.2. Cell permeabilization and depolarization of the membrane

AMPs have many mechanism(s) to kill microbes: (1) inhibition of cell wall synthesis, (2) disruption of the cytoplasmic membrane, (3) binding to DNA and (4) inhibition of protein synthesis. Among these mechanisms, disruption of the cell membrane is the most common [4]. Therefore, the effect of scolopendin 2 on bacteria and fungi was analyzed by monitoring the uptake of SYTOX Green, a membrane-impermeable DNA-binding molecule [34]. When treated with scolopendin 2, BUF(6–21) and melittin, 27.2%, 2.2% and 81.7% of the *E. coli* O157 cells and 33.1%, 3.6% and 76.2% of the *C. albicans* cells exhibited an increase in fluorescence (Fig. 3). Cells treated scolopendin 2 and melittin indicated a significant increase in fluorescence intensity. These results show that the bacterial and fungal cell membranes were permeabilized by the peptides.

The ability of scolopendin 2 to disrupt bacterial and fungal membrane potentials was investigated using $DiBAC_4(3)$, which binds to the cytoplasmic membrane of cells and allows estimation of the membrane potential [24]. Compared with untreated cells, 14.9%, 1.4% and 55.0% of *E. coli* O157 cells and 21.2%, 6.7% and 78.2% of *C. albicans* cells exposed to scolopendin 2, BUF(6–21) and melittin, respectively, showed an increase in fluorescence intensity (Fig. 4). Peptide-treated cells showed an accumulation of $DiBAC_4(3)$, indicating that scolopendin 2 caused depolarization of the membrane. The results of scolopendin 2 implied a membrane active mechanism of this peptide, whereas for BUF(6–21)

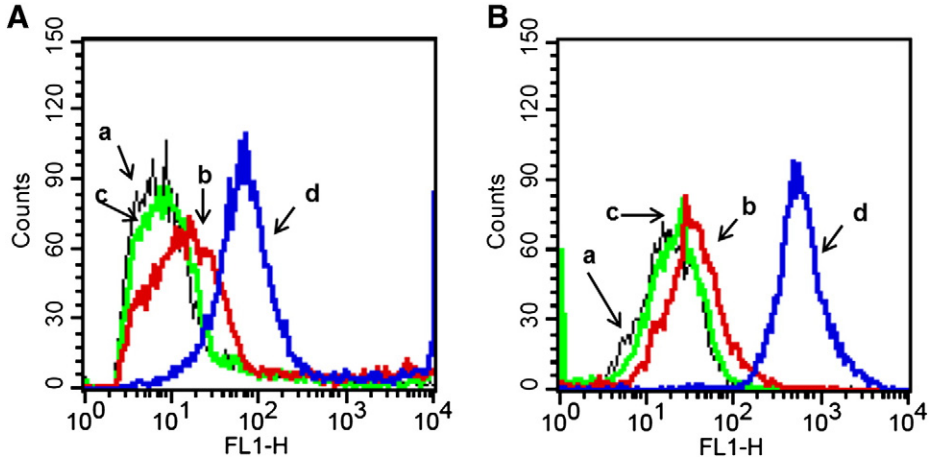

Fig. 3. Membrane permeabilization of (A) *E. coli* O157 and (B) *C. albicans*, detected by SYTOX Green fluorescence. The cells were treated with scolopendin 2, BUF(6–21) or melittin at the MIC. (a) Control, (b) scolopendin 2, (c) BUF(6–21), (d) melittin.

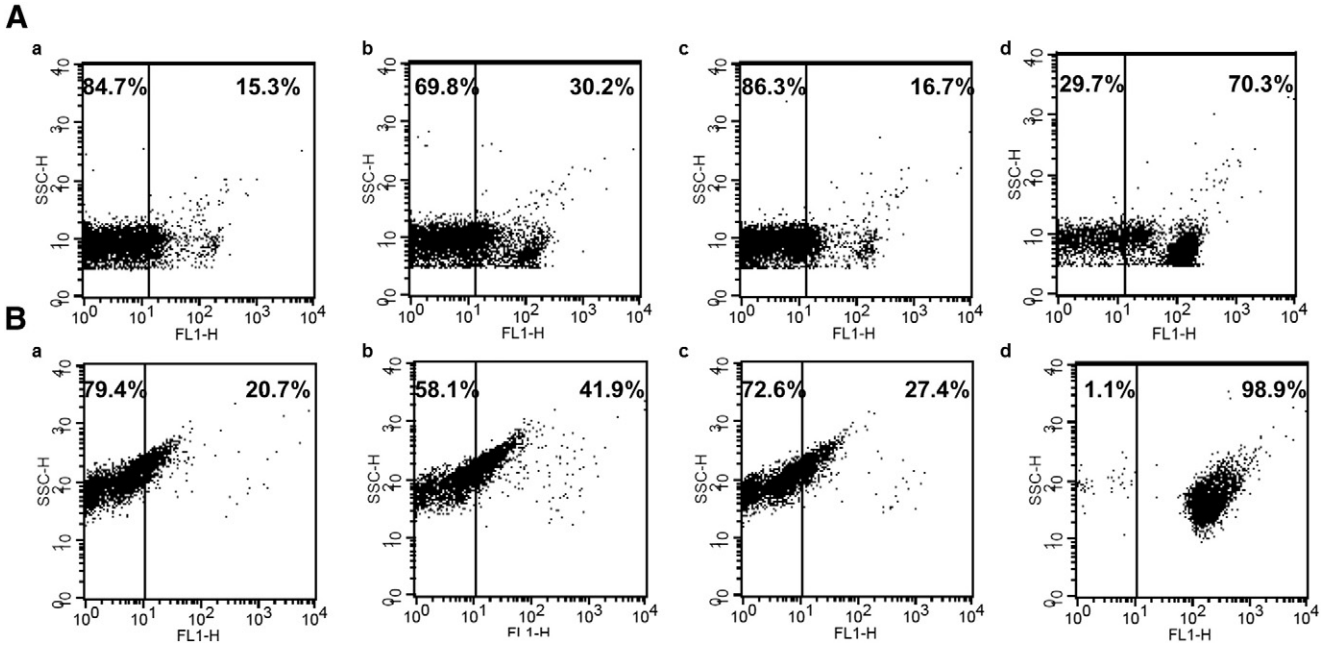

Fig. 4. Flow cytometric analysis of $DiBAC_4(3)$ staining after incubation of (A) *E. coli* O157 and (B) *C. albicans* with the MIC of the peptides. (a) Control, (b) scolopendin 2, (c) BUF(6–21), (d) melittin.

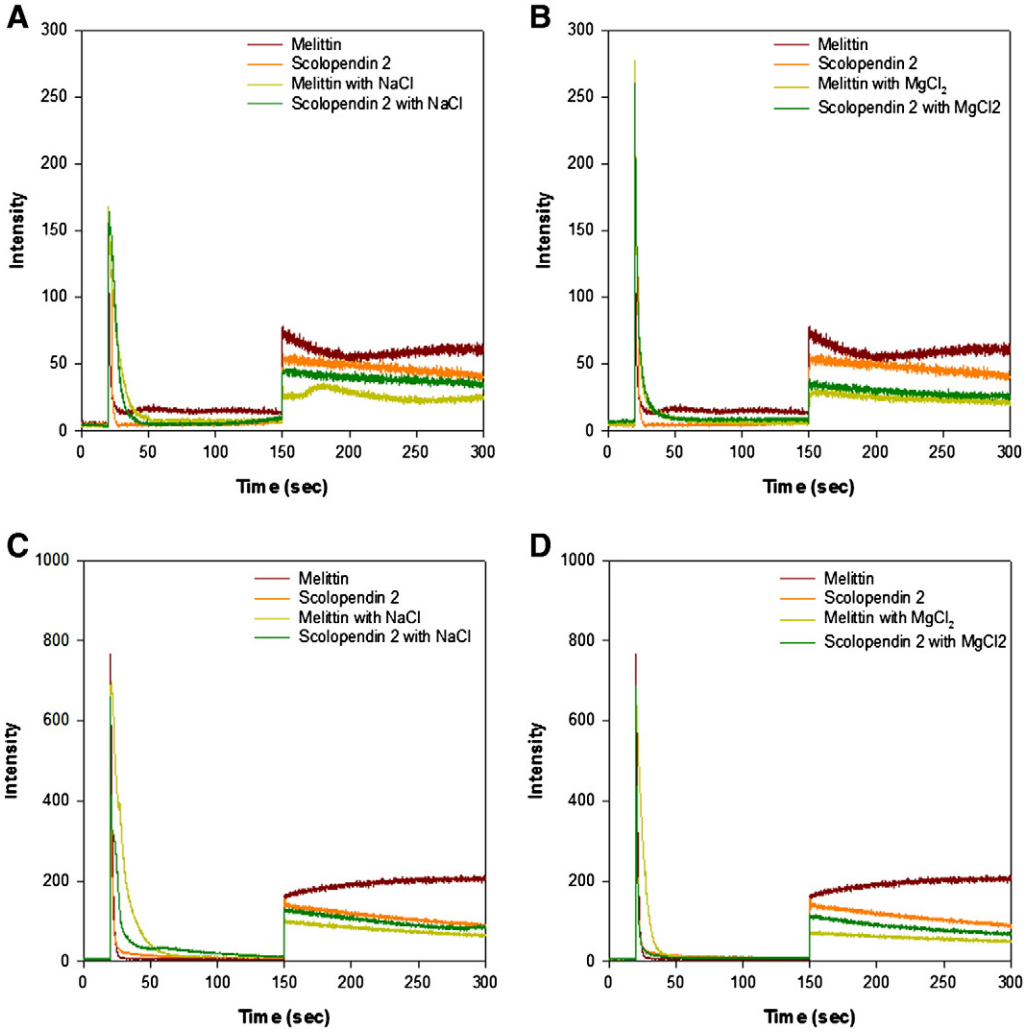

Fig. 5. Depolarization of *E. coli* O157 (A–B) and *C. albicans* (C–D) cell membranes were detected using $DiSC_3(5)$. $DiSC_3(5)$ was added at $t = 20$ s. After internalization of the probe, at $t = 150$ s, the MIC of scolopendin 2 or melittin was added and changes in fluorescence were monitored (excitation, 622 nm; emission, 670 nm). (A, C) Peptides with 150 mM NaCl; (B, D) peptides with 1 mM $MgCl_2$.

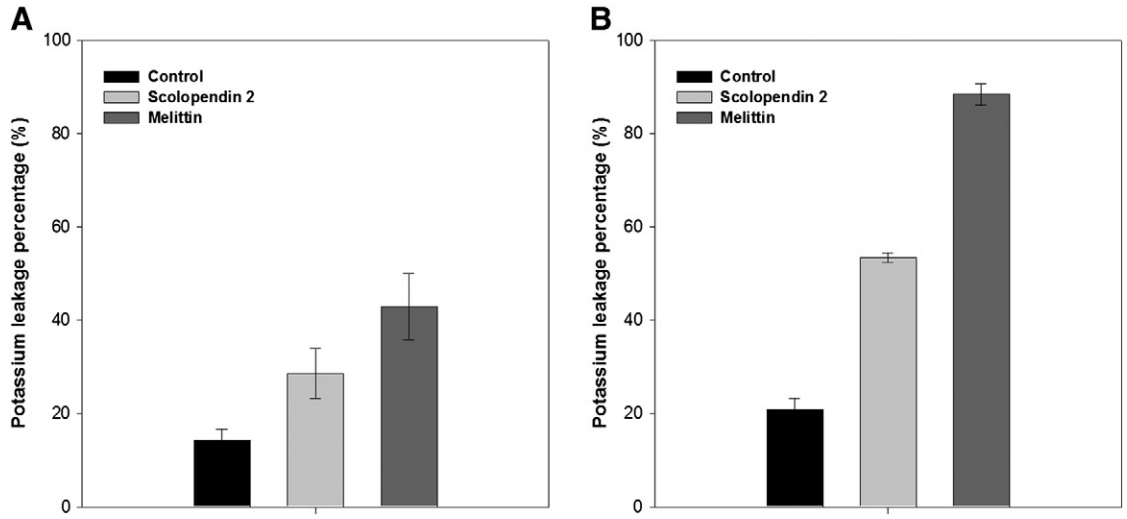

Fig. 6. Potassium leakage after incubation of (A) *E. coli* O157 and (B) *C. albicans* cells with the MIC of scolopendin 2 or melittin. The error bars represent the standard deviation.

the mechanism was not clearly identified. Accordingly, only melittin was used as a membrane-active control peptide in subsequent experiments.

When $DiSC_3(5)$, a potential-dependent distributional fluorescent dye [25], was added to cell suspensions (for 20 s), it was taken up and concentrated in the membrane, resulting in a steady baseline of fluorescence intensity. After quenching of the fluorescence of $DiSC_3(5)$, treatment with scolopendin 2 (for 150 s) led to a further increase in fluorescence intensity, albeit less than that observed with melittin. Moreover, the peptide activity decreased in the presence of 150 mM NaCl or 1 mM $MgCl_2$ (Fig. 5). These results show that scolopendin 2 can disrupt the cytoplasmic membrane and that its activity is inhibited by salt-dependent manner.

3.3. Release of intracellular potassium

To further investigate membrane damage, peptide-induced potassium release was measured using a potassium-sensitive electrode. Potassium efflux induced by scolopendin 2 was less than that induced by melittin. Potassium ion leakage from untreated *E. coli* O157 and *C. albicans* cells was 14.3% and 20.9%, respectively, while leakage from *E. coli* O157 and *C. albicans* cells treated with scolopendin 2 was 28.6% and 53.5%, respectively. In comparison, melittin-treated *E. coli* O157 and *C. albicans* cells leaked 42.9% and 88.4% of their potassium ions, respectively (Fig. 6). These results suggest that scolopendin 2 induces intracellular leakage.

3.4. Leakage of calcein from model membranes

To further investigate the membrane-active mechanism of scolopendin 2, artificial membranes were prepared and the extent of membrane damage induced by the peptides was measured. A self-quenching concentration of calcein was encapsulated in GUVs composed of PE/PG (3:1, w/w), which mimicked the inner membrane of *E. coli*, or PC/PE/PI/ergosterol (5:4:1:2, w/w/w/w), which mimicked the outer cell membrane of *C. albicans* [27]. Using inverted microscopy, we observed the changes in fluorescence from the two kinds of GUVs after the addition of peptide. Treatment with scolopendin 2 or melittin remarkably diminished the fluorescence of both GUVs. No changes were observed in the fluorescence intensity of control GUVs (Fig. 7). These results show that scolopendin 2 induced calcein leakage from GUVs, indicating that the structure of the liposomes was substantially disrupted.

3.5. FITC-dextran release by pore formation

To evaluate the size of the pores created by scolopendin 2 in the *E. coli* O157 and *C. albicans* membranes, the efflux of variably sized fluorescent molecules through the model membranes was observed. After the addition of scolopendin 2 to the model membranes, efflux of FD 4 (Stokes–Einstein radius = 1.4 nm), FD 10 (Stokes–Einstein radius = 2.3 nm), FD 20 (Stokes–Einstein radius = 3.3 nm) [35], and FD 40 (Stokes–Einstein radius = 4.8 nm) [36] from the liposomes was detected. However, no efflux from liposomes with encapsulated FD 70 (Stokes–Einstein radius = 5.0 nm) was observed. These results suggest that the size of the pores induced by scolopendin 2 was between 4.8 nm and 5.0 nm (Fig. 8).

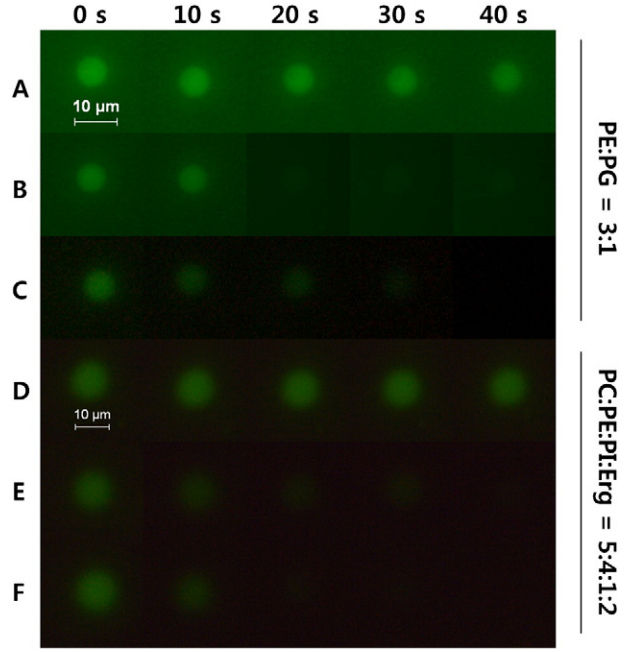

Fig. 7. Fluorescence from calcein-containing GUVs in the presence of the peptides at 0, 10, 20, 30, and 40 s. (A, D) Photobleaching, (B, E) scolopendin 2, (C, F) melittin. The bar represents 10 μm.

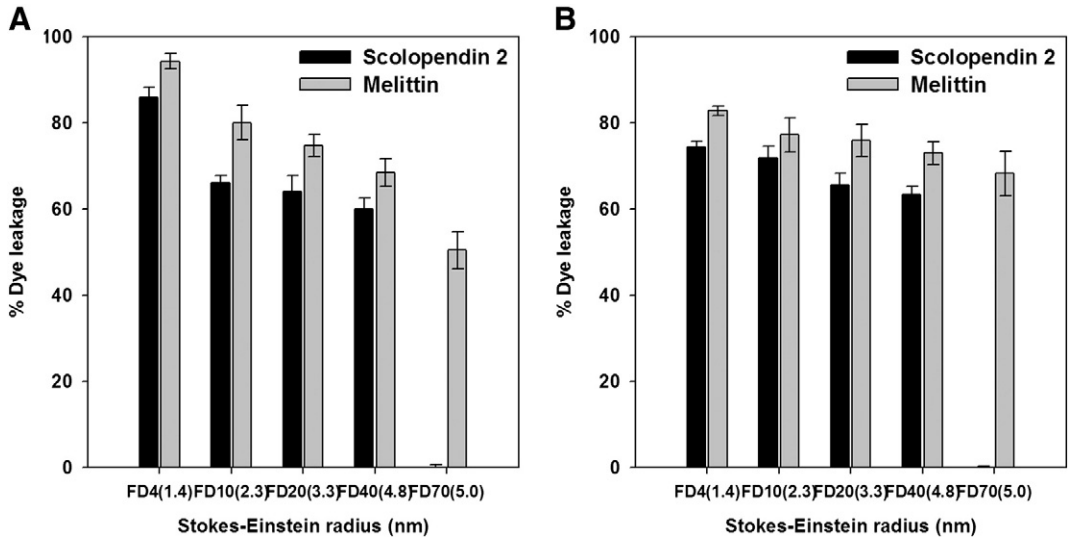

Fig. 8. FITC-dextran leakage from PE/PG (3:1, w/w) and PC/PE/PI/ergosterol (5:4:1:2, w/w/w/w) LUVs induced by the scolopendin 2 and melittin. (A) *E. coli* O157, (B) *C. albicans*. The leakage of FD70 from LUVS was not shown. The error bars represent the standard deviation of three independent experiments, each performed three times.

4. Discussions

AMPs from various organisms have been reported. Their amino acid composition, structure, net charge, and size are perceived to be significant properties that allow them to bind to or insert themselves into microbial pathogens, thus bringing about antimicrobial action through various mechanisms [5]. In a previous study, we identified scolopendin 1, an AMP from *S. s. mutilans*, by the same methods used in the present study; this AMP exerts its antifungal effect by triggering the apoptotic pathway [12]. In contrast, the peptide identified in this work, designated scolopendin 2, affects cell membranes. Scolopendin 2 was found to have sequence similarity with known antimicrobial peptides, including buforin 2, which targets nucleic acids without causing cell lysis [31,37]; temporins, which are known to disrupt the cytoplasmic membrane [5]; and CPF-AM4, from the caerulein-precursor fragment peptide family, which also shows antibacterial activity [32]. Before exploring the antimicrobial potential of scolopendin 2, we examined its secondary structure. CD spectroscopy showed that scolopendin 2 has an α-helical properties; such properties often have critical roles for microorganisms.

Generally, AMPs are classified into five groups based on their structure: peptides with α-helical structure; cysteine-rich peptides; peptides with β-sheet structure; peptides rich in histidine, arginine, and proline; and peptides with uncommon or modified amino acids. Among these classes, AMPs with α-helical properties are the most common [18]. Based on its structure, scolopendin 2 was considered a potential AMP. Therefore, we tested its antimicrobial activity and found that it was effective against morbific Gram-positive and Gram-negative bacteria, including antibiotic-resistant bacteria, and fungi. Among the susceptible strains, *E. coli* O157 and *C. albicans* were selected as model pathogenic microorganisms for further experiments [38,39]. Although scolopendin 2, BUF(6–21) had weaker antimicrobial activity than melittin, it showed no hemolytic effect on human erythrocytes. BUF(6–21) is a synethetic analog of buforin 2 with the same length as scolopendin 2 and only two differences in the amino acid sequence, I15V and G16H. Its antimicrobial activity was reported previously but the mechanism was so far not studied [31].

Potential modes of action of AMPs include fatal depolarization of the normally polarized membrane, formation of physical pores, scrambling of the usual distribution of lipids between the leaflets of the bilayer, and damage to critical intracellular targets. Cell death is induced by leakage of cellular contents and disturbance of membrane functions [37]. We considered it likely that a cationic peptide would damage plasma membranes. Therefore, to identify the mode(s) of action of scolopendin 2, we observed the effect of this peptide on bacterial and fungal plasma membranes. When cells are incubated with SYTOX Green, a fluorescent dye that intercalates with DNA but cannot cross intact cell membranes, an increase in fluorescence indicates cell death via membrane permeabilization [21] and breach of the plasma membrane [34]. Scolopendin 2 affected microbial cells by damaging their membranes and thus enhancing membrane permeability.

An increase in plasma membrane permeability can disrupt intracellular electrochemical gradients [40]. Using $DiBAC_4(3)$ and $DiSC_3(5)$, indicators of membrane potential, we showed that the membranes of cells exposed to scolopendin 2 were depolarized. Antimicrobial mechanisms that target the intracellular matrix cause little or no depolarization of membranes [20]. Therefore, we anticipated that the mechanism of scolopendin 2 did not involve inhibition of proteins or nucleic acids. BUF(6–21) was showed little depolarization and membrane permeability and it seems that the mechanism is not membrane related. Therefore, we used melittin as a positive control for comparing activity of the mode of action. Furthermore, membrane depolarization was reduced under physiological conditions in the presence of salt. As reported previously, a high sodium chloride concentration inhibits the antimicrobial activity of AMPs, and other salts, such as those with divalent ions, are even more inhibitory. Disruption of the interaction between the negatively charged membrane and the positively charged peptide is considered the cause of inhibition and is dependent on ionic strength [41]. The fact that scolopendin 2 was less susceptible to salt inhibition than melittin, which has a higher net charge, is a sign that this hypothesis is correct.

The potassium ion gradient is an important determinant of cell growth and survival because of its role in regulating cytoplasmic pH and cell structure [42]; therefore, a loss of cytoplasmic potassium would lead to cell death in bacteria and fungi [43,44]. Leakage of potassium ions has been used to determine membrane lytic events in bacteria and yeast because the internal ionic environment in prokaryotic and eukaryotic cells is usually potassium-rich [45]. The loss of the potassium gradient across the cell membrane, indicated by membrane depolarization, is an outcome of membrane damage and increased membrane permeability. The results of our study indicate that scolopendin 2 affects membrane integrity, leading to altered potassium efflux and subsequent depolarization of microbial membranes.

Positively charged peptides accumulate on anionic microbial cell surfaces containing acidic polymers and subsequently contact the cytoplasmic membrane [46]. Membrane permeabilization and depolarization by AMPs causes disruption of the bilayer, inducing the formation

of micelles, transmembrane pores, and toroidal pores [40,47]. To better understand the membrane-active mechanism of scolopendin 2, we used GUVs containing calcein. These GUVs mimicked the phospholipid composition of *E. coli* and *C. albicans* cell membranes. Morphological changes in artificial membranes allow the study of structural and physical changes during interactions with antimicrobial agents such as AMPs [48,49]. Changes in fluorescence are attributed to structural perturbation of the model membrane after interaction with these agents [11]. We observed that the fluorescence from liposomes gradually decreased, indicating that the fluorescent probes were escaping through pores in the liposomes. The liposomes did not shrink or collapse into micelles. These results indicate that the membrane-active mechanism of scolopendin 2 lies in pore formation within bacterial and fungal membranes.

To determine the size of the pores induced by scolopendin 2, we observed the efflux of FITC-dextrans, water-soluble fluorescent molecules with varying sizes, from LUVs. The pores induced by the peptide facilitated the efflux of FD 40 but not FD 70, indicating that the diameter of the pores in both types of liposomes used in this experiment was at least 4.8 nm but less than 5.0 nm. Melittin induces toroidal pores with a diameter of 3.0–5.0 nm [36] and allows passage of molecules of up to tens of kilodaltons at the micromolar scale [50]. Likewise, pores induced by scolopendin 2 seemed to permit transmission of small molecules or monatomic ions such as potassium. Migration of larger molecules such as glucose is anticipated.

In conclusion, scolopendin 2 was identified as a cationic AMP from *S. s. mutilans* that exhibits antimicrobial activities without causing hemolysis of human erythrocytes. Scolopendin 2 has a different mechanism of action than scolopendin 1, a previously identified AMP from the same centipede. Its membrane-active mechanism leads to the formation of pores in microbial plasma membranes, subsequent leakage of cytoplasmic matrix components, and consequent membrane depolarization, ultimately resulting in microbial cell death. These findings suggest that scolopendin 2 is a valuable source of AMP for human health and could be useful in area of food, cosmetic or pharmaceutical applications.

Acknowledgements

This work was supported by a grant from the Next-Generation BioGreen 21 Program (no. PJ008158), Rural Development Administration, Republic of Korea.

References

[1] A.J. Huh, Y.J. Kwon, "Nanoantibiotics": a new paradigm for treating infectious diseases using nanomaterials in the antibiotics resistant era, J. Control. Release 156 (2011) 128–145.
[2] J. Davies, D. Davies, Origins and evolution of antibiotic resistance, Microbiol. Mol. Biol. Rev. 74 (2010) 417–433.
[3] G.D. Wright, Bacterial resistance to antibiotics: enzymatic degradation and modification, Adv. Drug Deliv. Rev. 57 (2005) 1451–1470.
[4] L.T. Nguyen, E.F. Haney, H.J. Vogel, The expanding scope of antimicrobial peptide structures and their mode of action, Trends Biotechnol. 29 (2011) 464–472.
[5] M.L. Mangoni, Temporins, anti-infective peptides with expanding properties, Cell. Mol. Life Sci. 63 (2006) 1060–1069.
[6] A.T. Dossey, Insects and their chemical weaponry: new potential for drug discovery, Nat. Prod. Rep. 27 (2010) 1737–1757.
[7] A. Torres-Larios, G.B. Gurrola, F.Z. Zamudio, L.D. Possani, Hadrurin, a new antimicrobial peptide from the venom of the scolopin *Hadrurus aztecus*, Eur. J. Biochem. 267 (2000) 5023–5031.
[8] U. Theopold, O. Schmidt, K. Söderhäll, M.S. Dushay, Coagulation in arthropods: defense, wound closure and healing, Trends Immunol. 25 (2004) 289–294.
[9] H. Choi, J.S. Hwang, D.G. Lee, Identification of a Novel Antimicrobial Peptide, Scolopendin 1, Derived From Centipede *Scolopendra subspinipes mutilans* and Its Antifungal Mechanism, 2014., http://dx.doi.org/10.1111/imb.12124.
[10] W.K. You, Y.D. Sohn, K.Y. Kim, D.H. Park, Y. Jang, K.H. Chung, Purification and molecular cloning of a novel serine protease from the centipede, *Scolopendra subspinipes mutilans*, Insect Biochem. Mol. Biol. 34 (2004) 239–250.
[11] K. Peng, Y. Kong, L. Zhai, X. Wu, P. Jia, J. Liu, H. Yu, Two novel antimicrobial peptides from centipede venoms, Toxicon 55 (2010) 274–279.
[12] Y. Kong, Y. Shao, H. Chen, X. Ming, J.B. Wang, Z.Y. Li, J.F. Wei, A novel factor Xa-inhibiting peptide from centipedes venom, Int. J. Pept. Res. Ther. 19 (2013) 303–311.
[13] M.G. Grabherr, B.J. Haas, M. Yassour, J.Z. Levin, D.A. Thompson, I. Amit, Full-length transcriptome assembly from RNA-seq data without a reference genomes, Nat. Biotechnol. 29 (2011) 644–652.
[14] G. Pertea, X. Huang, F. Liang, V. Antonescu, R. Sultana, S. Karamycheva, TIGR gene indices clustering tools (TGICL): a software system for fast clustering of large EST datasets, Bioinformatics 19 (2003) 651–652.
[15] C. Iseli, C.V. Jongeneel, P. Bucher, ESTScan: a program for detecting, evaluating, and reconstructing potential coding regions in EST sequences, Proc. Int. Conf. Intell. Syst. Mol. Biol. (1999) 138–148.
[16] P. Rice, I. Longden, A. Bleasby, EMBOSS: the European molecular biology open software suite, Trends Genet. 16 (2000) 276–277.
[17] E. Lee, J.K. Kim, S. Shin, K.W. Jeong, A. Shin, J. Lee, D.G. Lee, J.S. Hwang, Y. Kim, Insight into the antimicrobial activities of coprisin isolated from the dung beetle, *Copris tripartitus*, reveled by structure–activity relationships, Biochim. Biophys. Acta 1828 (2013) 271–283.
[18] J. Lee, H. Choi, J. Cho, D.G. Lee, Effects of positively charged arginine residues on membrane pore forming activity of Rev-NIS peptide in bacterial cells, Biochim. Biophys. Acta 1808 (2011) 2421–2427.
[19] CLSI, Clinical and Laboratory Standards Institute Performance Standards for Antimicrobial Susceptibility Testing, Fifteenth ed. Wayne, PA, 2005.
[20] P. Wang, J.K. Bang, H.J. Kim, J.K. Kim, Y. Shin, Antimicrobial specificity and mechanism of action of disulfide-removed linear analogs of the plant-derived Cys-rich antimicrobial peptide Ib-AMP1, Peptides 30 (2009) 2144–2149.
[21] F.C. Mortimer, D.J. Mason, V.A. Gant, Flow cytometric monitoring of antibiotic-induced injury in *Escherichia coli* using cell-impermeant fluorescent probes, Antimicrob. Agents Chemother. 44 (2000) 676–681.
[22] S. Lüders, F. David, M. Steinwand, E. Jordan, M. Hust, S. Dübel, E. Franco-Lara, Influence of the hydromechanical stress and temperature on growth and antibody fragment production with *Bacillus megaterium*, Appl. Microbiol. Biotechnol. 91 (2011) 81–90.
[23] E.C. Veerman, M. Valentijn-Benz, K. Nazmi, A.L. Ruissen, E. Walgreen-Weterings, J. van Marle, A.B. Doust, W. van't Hof, J.G. Bolscher, A.V. Amerongen, Energy depletion protects *Candida albicans* against antimicrobial peptides by rigidifying its cell membrane, J. Biol. Chem. 282 (2007) 18831–18841.
[24] S.C. Park, M.H. Kim, M.A. Hossain, S.Y. Shin, Y. Kim, L. Stella, Y. Park, K.S. Hahm, Amphipathic alpha-helical peptide, HP (2–20), and its analogues derived from *Helicobacter pylori*: pore formation mechanism in various lipid compositions, Biochim. Biophys. Acta 1778 (2008) 229–241.
[25] S.D. Cox, J.E. Gustafson, C.M. Mann, J.L. Markham, Y.C. Liew, R.P. Hartiland, H.C. Bell, J.R. Warmington, S.G. Wyllie, Tea tree oil causes K^+ leakage and inhibits respiration in *Escherichia coli*, Lett. Appl. Microbiol. 26 (1998) 355–358.
[26] P. Kanmani, S.T. Lim, Synthesis and characterization of pullulan-mediated silver nanoparticles and its activities, Carbohydr. Polym. 97 (2013) 421–428.
[27] A. Makovitzki, D. Avrahami, Y. Shai, Ultrashort antibacterial and antifungal lipopeptides, Proc. Natl. Acad. Sci. U. S. A. 103 (2006) 15997–16002.
[28] M.I. Angelova, D.S. Dimitrov, Liposome electroformation, Faraday Discuss. Chem. Soc. 81 (1986) 303–311.
[29] M.I. Angelova, S. Sloeau, P. Meleard, J.F. Faucon, P. Bothorel, Preparation of giant vesicles by external AC electric fields Kinetics and application, Prog. Collied Polym. Sci. 89 (1992) 127–131.
[30] F. Yoneyama, Y. Imura, K. Ohno, T. Zendo, J. Nakayama, K. Matsuzaki, K. Sonomoto, Peptide–lipid huge toroidal pore, a new antimicrobial mechanism mediated by a lactococcal bacteriocin, lactin Q, Antimicrob. Agents Chemother. 53 (2009) 3211–3217.
[31] C.B. Park, K.S. Yi, K. Matsuzaki, M.S. Kim, S.C. Kim, Structure–activity analysis of buforin II, a histone H2A-derived antimicrobial peptide: the proline hinge is responsible for the cell-penetrating ability of buforin II, Proc. Natl. Acad. Sci. U. S. A. 97 (2000) 8245–8250.
[32] J.M. Conlon, N. Al-Ghaferi, E. Ahmed, M.A. Meetani, J. Leprince, P.F. Nielsen, Orthologs of magainin, PGLa, procaerulein-derived, and proxenopsin-derived peptides from skin secretions of the octoploid frog *Xenopus amieti* (Pipidae), Peptides 31 (2010) 989–994.
[33] B. Skerlavaj, M. Benincasa, A. Risso, M. Zanetti, R. Gennaro, SMAP-29: a potent antibacterial and antifungal peptide from sheep leukocyte, FEBS Lett. 463 (1999) 58–62.
[34] F.H. Pilsczek, D. Salina, K.K. Poon, C. Fahey, B.G. Yipp, C.D. Sibley, S.M. Robbins, F.H. Green, M.G. Surette, M. Sugai, M.G. Bowden, M. Hussain, K. Zhang, P. Kubes, A novel mechanism of rapid nuclear neutrophil extracellular trap formation in response to *Staphylococcus aureus*, J. Immunol. 185 (2010) 7413–7425.
[35] C.M. Sandoval, B. Salzameda, K. Reyes, T. Williams, V.S. Hohman, L.A. Plesniak, Anti-obesity and anti-tumor pro-apoptotic peptides are sufficient to cause release of cytochrome c from vesicles, FEBS Lett. 581 (2007) 2463–5468.
[36] S.C. Park, M.H. Kim, M.A. Hossain, Y. Kim, L. Stella, J.D. Wade, Y. Park, K.S. Hahm, Amphipathic alpha-helical peptide, HP (2–20), and its analogues derived from *Helicobacter pylori*: pore formation mechanism in various lipid compositions, Biochim. Biophys. Acta 1778 (2008) 229–241.
[37] M. Zasloff, Antimicrobial peptides of multicellular organisms, Nature 415 (2002) 389–395.
[38] O. Habimana, E. Heir, S. Langsrud, A.W. Asli, T. Møretrø, Enhanced surface colonization by *Escherichia coli* O157:H7 in biofilms formed by an *Acinetobacter calcoaceticus* isolate from meat-processing environments, Appl. Environ. Microbiol. 76 (2010) 4557–4559.
[39] E. Lee, K.W. Jeong, J. Lee, A. Shin, J.K. Kim, J. Lee, D.G. Lee, Y. Kim, Structure–activity relationships of cecropin-like peptides and their interactions with phospholipid membrane, BMB Rep. 46 (2013) 282–287.

[40] K.A. Brogden, Antimicrobial peptides: pore formers or metabolic inhibitors in bacteria? Nat. Rev. Microbiol. 3 (2005) 238–250.
[41] D. Ma, C. Zhou, M. Zhang, Z. Han, Y. Shao, S. Liu, Functional analysis and induction of four novel goose (*Anser cygnoides*) avian β-defensin in response to *Salmonella eneritidis* infection, Comp. Immunol. Microbiol. Infect. Dis. 35 (2012) 197–207.
[42] T.P. Roosild, S. Castronovo, J. Healy, S. Miller, C. Pliotas, T. Rasmussen, W. Bartlett, S.J. Conway, I.R. Booth, Mechanism of ligand-gated potassium efflux in bacterial pathogens, Proc. Natl. Acad. Sci. U. S. A. 107 (2010) 19784–19789.
[43] A. Peña, N.S. Sánchez, M. Calahorra, Effects of chitosan on *Candida albicans*: conditions for its antifungal activity, Biomed. Res. Int. 2013 (2013) 527549.
[44] D. Bolintineau, E. Hazrati, H.T. Davis, R.I. Lehrer, Y.N. Kaznessis, Antimicrobial mechanism of pore-forming protegrin peptides: 100 pore to kill *E. coli*, Peptides 31 (2010) 1–8.
[45] D.S. Orlve, T. Nguyen, R.I. Lehrer, Potassium release, a useful tool for studying antimicrobial peptides, J. Microbiol. Methods 49 (2002) 325–328.
[46] R.E. Hancock, H.G. Sahl, Antimicrobial and host-defense peptides as new anti-infective therapeutic strategies, Nat. Biotechnol. 24 (2006) 1551–1557.
[47] M. wenzel, B. Kohl, D. Münch, N. Raatschen, H.B. Albada, L. Hamoen, N. Metzler-Nolte, H.G. Sahl, J.E. Bandow, Proteomic response of *Bacillus subtilis* to lantibiotics reflects differences in interaction with the cytoplasmic membrane, Antimicrob. Agents Chemother. 56 (2012) 5749–5757.
[48] Y. Tamba, H. Ariyama, V. Levadny, M. Yamazaki, Kinetic pathway of antimicrobial peptide magainin 2-induced pore formation in lipid membranes, J. Phys. Chem. B 114 (2010) 12018–12026.
[49] Y. Tamba, T. Tanaka, T. Yahagi, Y. Yamashita, M. Yamazaki, Stability of giant unilamellar vesicles and large unilamellar vesicles of liquid-ordered phase membranes in the presence of Triton X-100, Biochim. Biophys. Acta 1667 (2004) 1–6.
[50] M.T. Lee, T.L. Sun, W.C. Hung, H.W. Huang, Process of inducing pores in membranes by melittin, Proc. Natl. Acad. Sci. U. S. A. 110 (2013) 14243–14248.